

# The Analysis of Vibration Signals of Critical Points of the Bus Body Frame

Artūras Kilikevičius<sup>1\*</sup>, Kristina Kilikevičienė<sup>2</sup>, Antanas Fursenko<sup>3</sup>, Jonas Matijošius<sup>2</sup>

<sup>1</sup> Institute of Mechanical Science, Vilnius Gediminas Technical University, LT-03224 Vilnius, Basanavičiaus St. 28, Lithuania

<sup>2</sup> Department of Automobile Transport, Vilnius Gediminas Technical University, LT-03224 Vilnius, Basanavičiaus str. 28, Lithuania

<sup>3</sup> Department of Mechanical Engineering, Vilnius Gediminas Technical University, LT-03224 Vilnius, Basanavičiaus str. 28, Lithuania

\* Corresponding author, e-mail: [arturas.kilikevicius@vgtu.lt](mailto:arturas.kilikevicius@vgtu.lt)

Received: 03 January 2018, Accepted: 04 July 2018, Published online: 17 December 2019

## Abstract

In this paper, authors have investigated wave distribution caused by the mechanical structure of a passenger bus body frame and its parameters based on the theory of covariance functions. Authors have measured the intensity of vibrations at fixed points. Time scale analyses were conducted based on data arrays (matrixes). The estimates of covariance functions clearly showed that changes in the state of the bus mechanical structure invariably impact changes of the intensity of vibration signals at the relevant points. In the analysis, software Matlab 7 was applied.

## Keywords

bus body, vibrations, covariance function, quantization interval

## 1 Introduction

Bus utilization specialists keep searching for innovative methods and actions to simplify the technical inspection of bus body frame solidity. The aim of these investigations is to ensure the reliability and the passenger comfort of transportation by bus. Reducing the time and cost of vehicle maintenance is possible by non-destructive testing. In this paper, an analysis of digital signals of a mechanical object's vibration parameters is carried out upon the application of the theory of random functions (Kilikevičienė et al., 2015).

The theoretical model is based on the concept of stationary random function. The authors have taken into account that the errors of measuring the vibration parameters are random and the average error  $M\Delta = const \rightarrow 0$ , their dispersion  $D\Delta = const$ , and covariance function of digital signals depends only on the difference between the arguments, i.e. on the quantization interval on the time scale.

Estimates of the covariance functions of two vibration signals or the covariance functions of a single signal are calculated upon transformation. For processing the digital signals the theory of wavelet functions (Kardoulas et al., 1996; Eliason and McEwen, 1990; Hunt et al., 1993; Antoine, 2000; Dutkay and Jorgensen, 2004) were applied.

Wavelet analysis has recently been recognized as a tool for important applications in time series, function estimation and image analysis. According to the development in the most recent wavelet methods, the fundamentals of the field are not yet widely understood, and their practical application is hard to find. Wavelets are an increasingly and widely used tool in many applications of both signal and image processing. Applications in remote sensing include the combination of different resolution images, compression, and the provision of edge detection methods. Researcher Horgan (1998) reviewed the basic ideas of wavelets in order to represent information as signals; such as time series and images, and described how wavelet shrinkage is applied to smooth these signals. This was illustrated by the application of a synthetic aperture radar image.

The temporal dependence of a stationary stochastic process is characterized by its auto-covariance function or, alternatively by its Fourier transformed spectral density function. Data reconciliation can be used for filtering, to improve measurement reliability and precision, and it is also applicable for the estimation of unmeasured variables. These features make the process a valuable measurement tool. In these cases, strategic variables are only

measured with limited reliability or in some cases some variables were simply not measured due to technical or economic constraints (Hodouin and Flament, 1991; Mah, 1990; Narasimhan and Jordache, 2000; Romagnoli and Sanchez, 2000).

This paper analyses the digital signal estimates of bus body frame vibration, carried out upon application of random function theory.

## 2 A covariance model of vibration parameters

In this paper a theoretical model was applied, where the authors considered random errors in measurement. The trend of the measuring data was statistically eliminated. The authors have considered the random function and its average value  $M\{\phi(t)\} \rightarrow const$ , and covariance function depends only on the difference of arguments –  $K_\phi(\tau)$ . The auto-covariance function of a single data array or the cross-covariance function of two data arrays  $K_\phi(\tau)$  shall be written as follows (Skeivalas and Kizlaitis, 2008):

$$K_\phi(\tau) = \frac{1}{T-\tau} \int_0^{T-\tau} \delta\phi_1(u) \delta\phi_2(u+\tau) du, \quad (1)$$

Where  $\delta\phi_1(u), \delta\phi_2(u+\tau)$  is the centered values of vibration intensity measurements,  $u$  is vibration parameter,  $\tau = k \cdot \Delta$  is variable quantization interval,  $k$  is the number of units of measurement,  $\Delta$  is the value of a unit of measurement,  $T$  is time.

According to available data on measurements of vibration parameters, the estimate  $K'_\phi(\tau)$  of covariance function is calculated as follows:

$$K'_\phi(\tau) = K'_\phi(k) = \frac{1}{n-k} \sum_{i=1}^{n-k} \delta\phi_1(u_i) \delta\phi_2(u_{i+k}), \quad (2)$$

where  $n$  is the total number of discrete intervals.

Formula (Eq. (2)) may be applied in the form of an auto-covariance function or a cross-covariance function. When the function is an auto-covariance function, the arrays  $\phi_1(u)$  and  $\phi_2(u+\tau)$  are parts of single arrays, while when the function is a cross-covariance function, they are two different arrays. The estimate of a normed covariance function is:

$$R'_\phi(k) = \frac{K'_\phi(k)}{K'_\phi(0)} = \frac{K'_\phi(k)}{\sigma_\phi'^2}, \quad (3)$$

where  $\sigma'_\phi$  is the estimate of the standard deviation of a random function.

For elimination of the trends of columns in the  $i$ -th digital array of measurements, the following formulas are applied:

$$\delta\varphi_i = \varphi_i - e \cdot \bar{\varphi}_i^T = (\delta\varphi_{i1}, \dots, \delta\varphi_{im}), \quad (4)$$

where  $\delta\varphi_i$  is the  $i$ -th digital array of reduced values where a trend of column is eliminated;  $\varphi_i$  is the  $i$ -th array of the vibration intensity,  $e$  is a unit vector with the sizes  $(n \times 1)$ ;  $n$  is the number of lines in the  $i$ -th array,  $\bar{\varphi}_i$  is the vector of average values of columns in the  $i$ -th array,  $\delta\varphi_{ij}$  is the  $j$ -th column (vector) of the reduced values in the  $i$ -th array.

The vector of average values of columns in the  $i$ -th array is calculated according to the following formula:

$$\bar{\varphi}_i^T = \frac{1}{n} e^T \cdot \varphi_i = \frac{1}{n} \varphi_i^T \cdot e. \quad (5)$$

A realization of the random function of the  $j$ -th column of the  $i$ -th array of vibration intensity in form of vectors shall be expressed as follows:

$$\delta\varphi_{ij} = (\delta\varphi_{ij,1}, \dots, \delta\varphi_{ij,m}). \quad (6)$$

The estimate of the covariance matrix of the  $i$ -th array of wavelet intensity is expressed as follows:

$$K'(\delta\varphi) = \frac{1}{n-1} \delta\varphi_i^T \delta\varphi_i. \quad (7)$$

The estimate of covariance matrix of two arrays of vibration intensity is written as follows:

$$K'(\delta\varphi_i, \delta\varphi_j) = \frac{1}{n-1} \delta\varphi_i^T \delta\varphi_j, \quad (8)$$

where the sizes of  $\delta\varphi_i, \delta\varphi_j$  arrays should be the same.

The estimates  $K'(\delta\phi_i)$  and  $K'(\delta\phi_i, \delta\phi_j)$  of covariance matrixes are reduced into estimates of matrixes of correlation coefficients  $R'(\delta\phi_i)$  and  $R'(\delta\phi_i, \delta\phi_j)$  (Skeivalas et al., 2010; 2015):

$$R'(\delta\varphi_i) = D_i^{-1/2} K'(\delta\varphi_i) D_i^{-1/2}, \quad (9)$$

$$R'(\delta\varphi, \delta\varphi_j) = D_{ij}^{-1/2} K'(\delta\varphi_i, \delta\varphi_j) D_{ij}^{-1/2}, \quad (10)$$

where  $D_i, D_{ij}$  are the diagonal matrixes of members of principal diagonals in the estimates of covariance matrixes  $K'(\delta\phi_i)$  and  $K'(\delta\phi_i, \delta\phi_j)$ , respectively.

The accuracy of the calculated coefficients of correlation is defined by the standard deviation  $\sigma_r$ , and the value of the latter is assessed according to the following formula:

$$\sigma_r = \frac{1}{\sqrt{n}} (1-r^2), \quad (11)$$

where  $n = 8000$ ,  $r$  is the coefficient of correlation. The maximum value of the standard deviation is obtained when

the value of  $r$  is close to zero and in this case,  $\sigma_r' \approx 0.01$ , when  $r \approx 0.5$ , we obtain  $\sigma_r' \approx 0.008$ .

### 3 The results of the experiment and the analysis

The values of vibration signals were measured in 4 points of the frame of the bus upon the following three states:

1. Idle state of the bus engine;
2. Operating state of the bus engine;
3. Vertical shock excitation of the bus body, and measurement in the vertical direction.

The data arrays of measuring the relevant parameters of vibration signals were formed on measuring wavelets of the bus frame upon using the following devices:

Portable measurement data processing, storage and control equipment "3660-D" (Fig. 1(a)) from "Bruel and Kjar" company; Computer DEEL (Fig. 1(a)); Accelerometers 8344 (Fig. 1(b)).

Vectors of vibration signals were measured in the 4 points of the bus frame and measurement data arrays of

4 vectors were obtained for three states. The signals were fixed in the interval  $\tau_\Delta = 2.44140630 \cdot 10^{-4}$  s on the time scale. Each vector of an array included  $n = 16386$  values of vibration signals.

Wavelets were measured in certain points of the bus frame and the suspension (shown in Fig. 2) in a quiescent state (i.e. when the bus was not affected by external excitation), upon starting the engine and upon shock excitation. The measurements were carried out in the vertical position. In Fig. 3, the views of the measurement points are provided. The measurement results are presented in Fig. 4, Fig. 5 and Fig. 6 (b).

The data arrays for the three states of the bus obtained in the measurement data processing procedures were used to form two data groups, where the measurement data of two states of the bus were used in each group.

The first group was formed upon applying the data obtained:

- while the engine of the bus was in idle state;
- while the engine of the bus was in operating state.

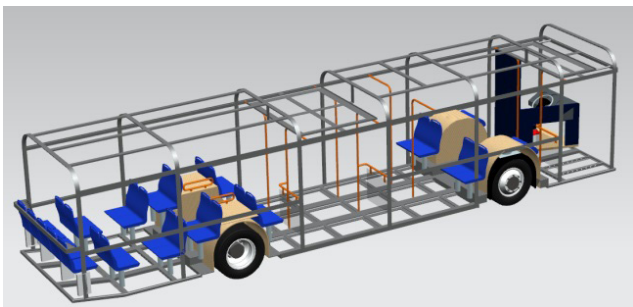


(a)

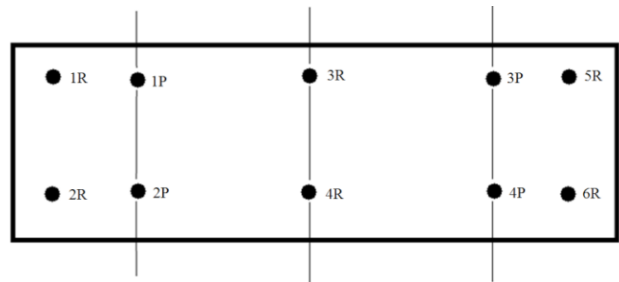


(b)

**Fig. 1** The tools for measuring the wavelet parameters: a) portable measurement data processing, storage and control equipment "3660-D" with DELL computer; b) accelerometer 8344



(a)



(b)

**Fig. 2** The scheme of the bus frame and the suspension wavelet measurement points: a) the view of the frame; b) the bottom view

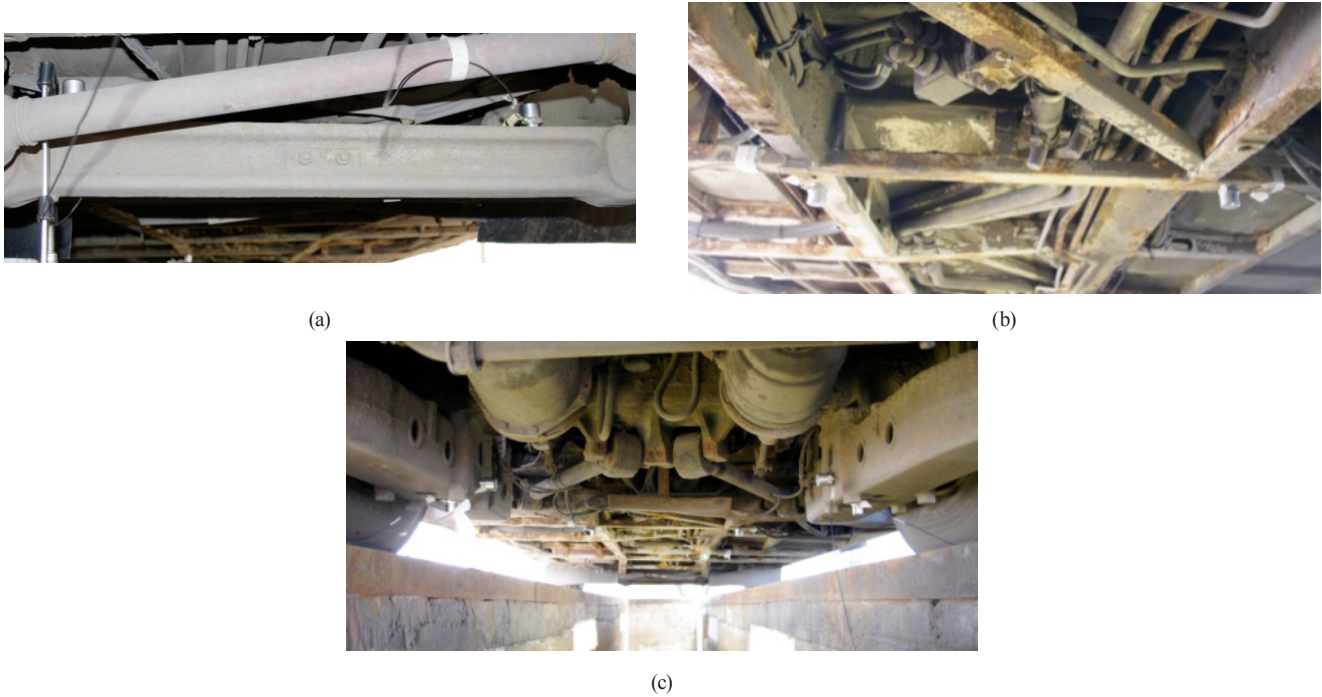


**Fig. 3** The bus frame and suspension wavelet measurement points: a) the points of the front suspension of the bus (Fig. 2, the points 1P and 2P); b) the points of the frame in the middle of the bus (Fig. 2, the points 3R and 4R); c) the points of the rear suspension of the bus (Fig. 2, the points 3P and 4P)

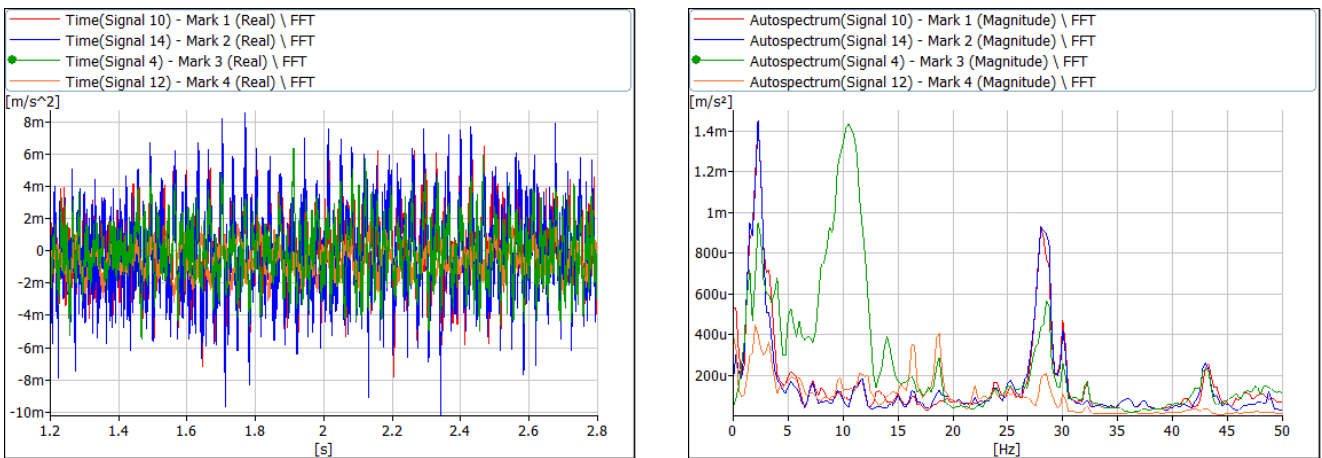


**Fig. 4** The diagrams of time signal of absolute wavelet vertical acceleration amplitude in the middle points of the frame (Fig. 2, the points 3R and 4R) and the suspension (Fig. 2, the points 1P and 4P) as well as the autospectrum signal in the idle state

The second group was formed upon applying the data obtained:

- during vertical shock excitation of the bus and measurement in the vertical direction has taken place;
- while the engine of the bus was in operating state.

The arrays of the measuring data were processed according to the custom software upon applying operators of Matlab 7 program package.

The values of quantization intervals of the normed covariance functions vary from 1 to  $n/2$ , where  $n = 16386$

– the number of lines (values) of the wavelet signal vectors in an array. An array of measuring wavelet signals consists of 4 vectors (columns) for each state of the vehicle, where each point of the vehicle surface corresponds to one vector of the measurement results. For each vector, the estimate  $K'_\varphi(\tau)$  of the normed covariance function  $K_\varphi(\tau)$  was calculated and 4 graphical expressions of the normed covariance functions were obtained for each state. In addition, the estimates of the normed cross-covariance functions  $K'_\varphi(\tau)$  according to the vectors of all 4 points and 56 graphical expressions of these were obtained.

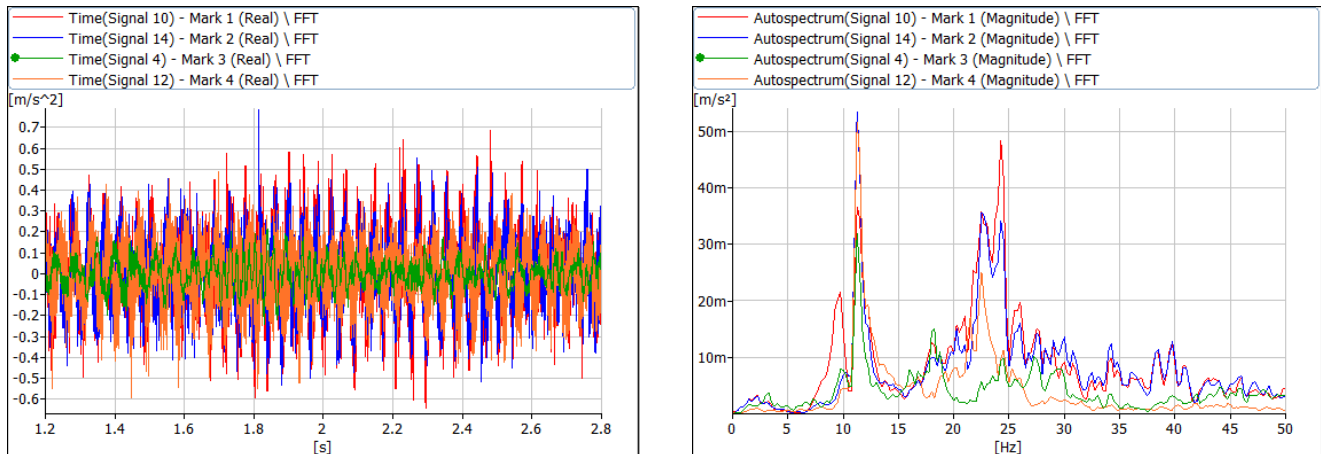


**Fig. 5** The diagrams of time signal of absolute wavelet vertical acceleration amplitude in the middle points of the frame (Fig. 2 above, the points 3R and 4R) and the suspension (Fig. 2 above, the points 1P and 4P) as well as the autospectrum signal when the engine is started

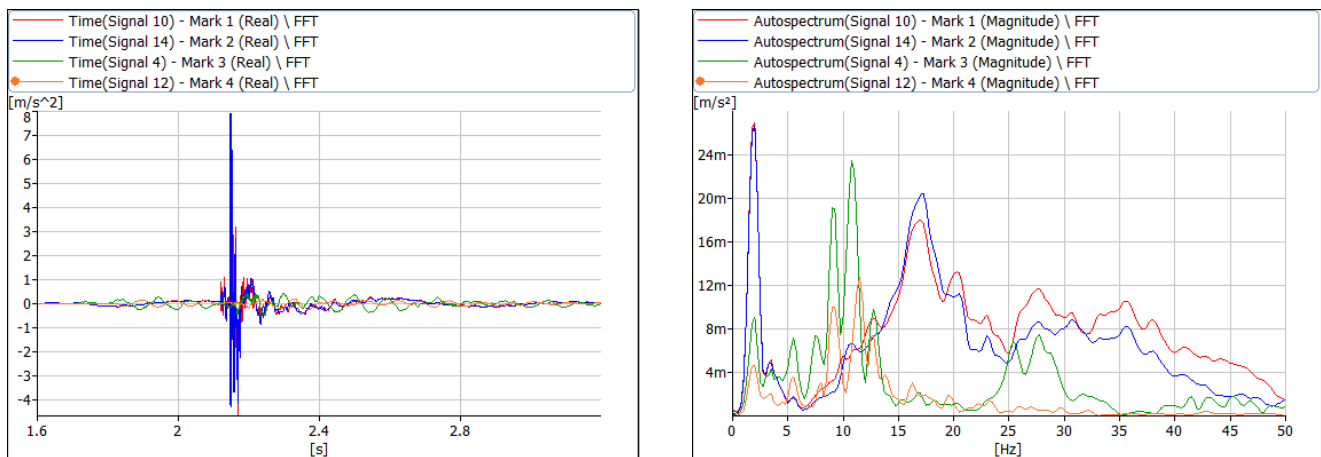


**Fig. 6** The diagrams of time signal of absolute wavelet vertical acceleration amplitude in the middle points of the frame (Fig. 2 above, the points 3R and 4R) and the suspension (Fig. 2 above, the points 1P and 4P) as well as the autospectrum signal upon a shock excitation in the middle of the bus

For measurements in each state, four points of the bus frame (3R, 4R, 1P, 4P) were used, and a vector of the measurement results was obtained for each point. Altogether, 4 measurement vectors were obtained for each state. In order to simplify numbering of the vectors, a new first in first out numeration (1, 2, 3, 4) was applied in the calculation procedures. When vectors for both states were united into one system, they were numbered (1, 2, 3, 4; 5, 6, 7, 8).

The normed auto-covariance functions have the maximum correlation coefficient  $r = 1.0$  when the quantization interval  $k = 0 (\tau_k = 0 s)$ .

Let's analyze the results of processing the first group of measurement data arrays. The expressions of the normed auto-covariance functions of vibration signals at the 4 pre-selected points of the mechanical structure of the vehicle (3R, 4R, 1P, 4P) in two states are of irregular "undamped"

periodical character and the values of their correlation coefficients vary in the range  $|r| \rightarrow 1.0 - 0.5 - 0.1$  at all values of quantization interval  $k$ . It is evident that the periodic character of the normed auto-covariance functions is a trace of the periodicity of the measured vibration signals.

The normed cross-covariance functions also become of irregular periodical character, and have small values of the correlation coefficients that vary in the range  $|r| \rightarrow 0.5 - 0.2 - 0.01$  at all values of quantization interval  $k$  in the both states of the bus. Several cross-covariance functions have the values of the correlation coefficients close to  $|r| \rightarrow 0.4 - 0.5$ , caused by the following vectors:

- 3R and 4R (the state 1),  $|r| \rightarrow 0.5 - 0.2$  ;
- 3R and 1P (the state 1),  $|r| \rightarrow 0.4 - 0.2$  ;
- 4R and 1P (the state 1),  $|r| \rightarrow 0.4 - 0.2$  ;
- 3R and 4R (the state 2),  $|r| \rightarrow 0.45 - 0.15$  .

So, when the vehicle frame is in an idle state and when the engine is operating, the cross correlation between the vibration signals of vectors of the points is low but the maximum values of the correlation coefficients for several vectors of points are  $|r| \rightarrow 0.4 - 0.5$ .

The most important graphical expressions of auto-covariance and cross-covariance functions of the first group vibration signals are shown in Figs. 7–11. Fig. 12 provides the graphical view of the generalized (spatial) correlation matrix of 8-vector array for 4 points of the vehicle in two states. The expression of the correlation matrix turns into a block of 8 pyramids where the values of correlation coefficients are shown as colors of the spectrum. The chromatic projection of the pyramids is shown in the horizontal plane.

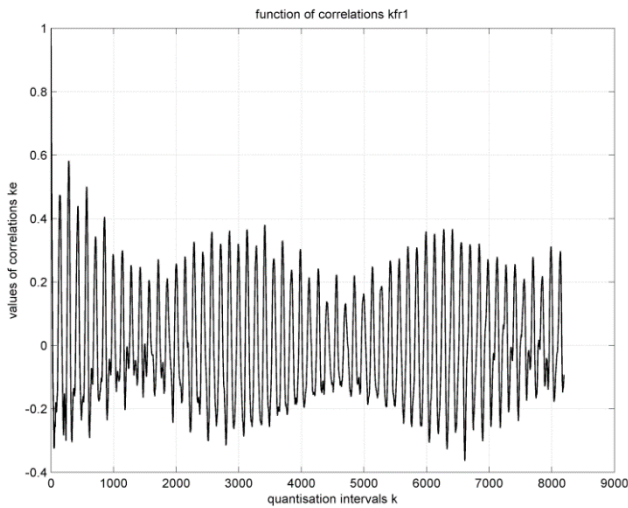


**Fig. 7** The normed auto-covariance function of the vibration signals at the point 3R when the engine is in idle state

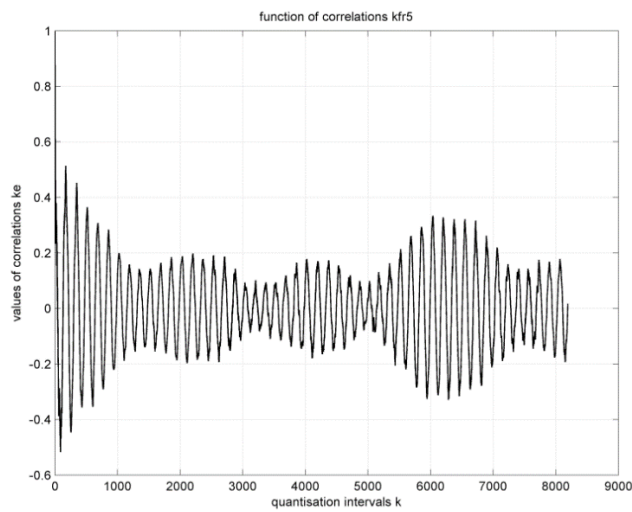


**Fig. 8** The normed auto-covariance function of the vibration signals at the point 3R when the engine is in operating state

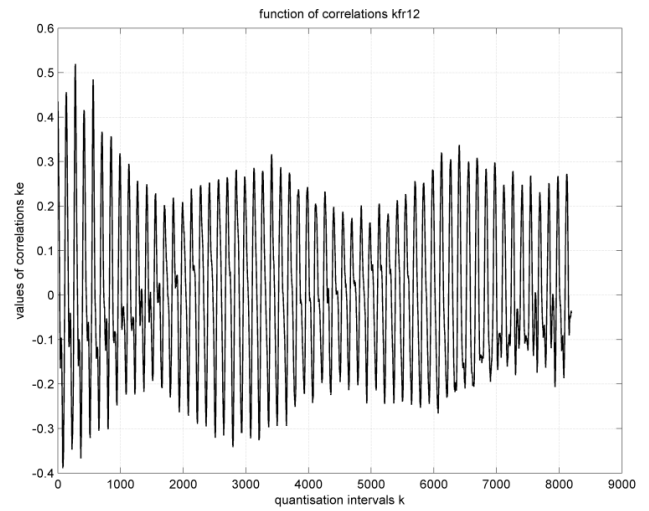


**Fig. 9** The normed cross-covariance function of the vibration signals at the points 3R and 4R when the engine is in idle state

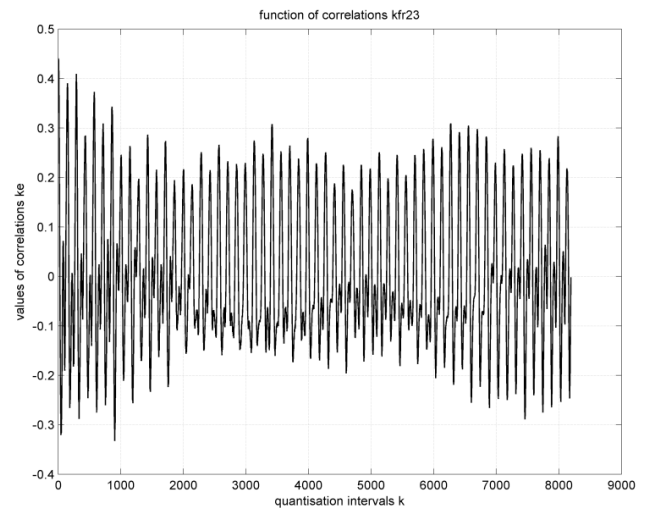


**Fig. 10** The normed cross-covariance function of the vibration signals at the points 4R and 1P when the engine is in idle state

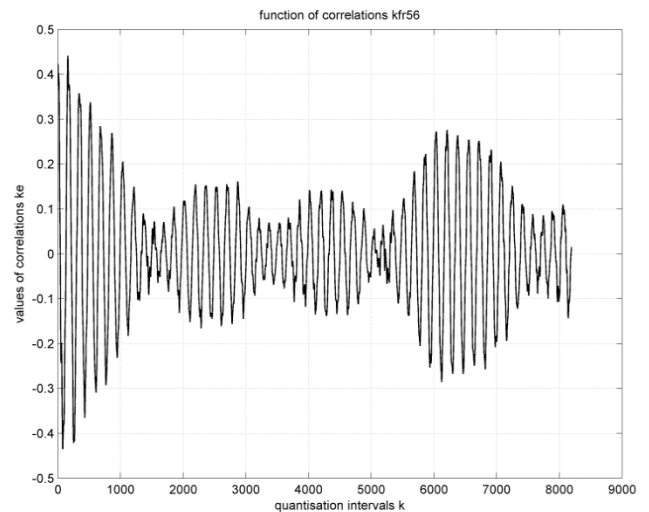


**Fig. 11** The normed cross-covariance function of the vibration signals at the points 3R and 4R when the engine is in idle state

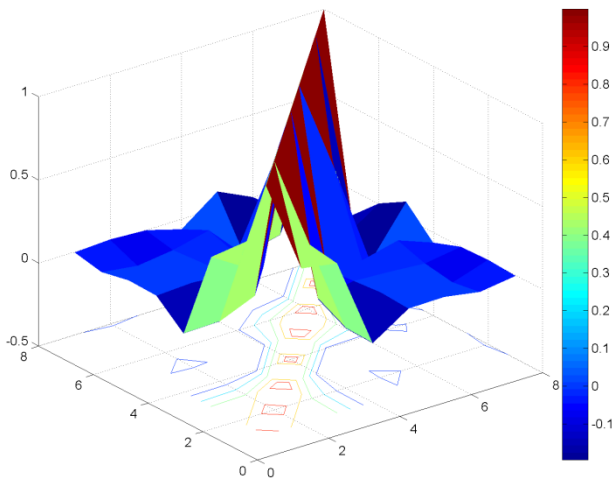


**Fig. 12** The graphical expression of the generalized (spatial) correlation matrix of the array of 8 vectors of 4 points of the bus body frame in two states

Let's analyze the results of processing the second group of measurement data arrays. The expressions of the normed auto-covariance functions for 4 points of the vehicle body frame (3R, 4R, 1P, 4P) in the second state are of low periodicity, and the values of correlation coefficients decrease from  $|r| \rightarrow 1.0$  to  $|r| \rightarrow 0.1$ . In the first state, the estimates of auto-covariance functions decrease from  $r \rightarrow 1.0 (k \rightarrow 0)$  to  $r \rightarrow 0$  at the values of quantization interval  $k \rightarrow 5000 (\tau_k \rightarrow 1.2s)$ .

The estimates of normed cross-covariance functions become low at all values of quantization interval  $k$  in both states of the bus and the correlation coefficient  $r \rightarrow 0$  at  $k \rightarrow 5000 (\tau_k \rightarrow 1.22s)$ . The estimates of several cross-covariance functions are somewhat higher, when  $|r| \rightarrow 0.7 - 0.45$  and it is caused by the vectors of vibration signals at the relevant points:

- 3R and 4R (the state 1),  $|r| \rightarrow 0.7 - 0.1$  ;
- 1P and 4P (the state 1),  $|r| \rightarrow 0.5 - 0.0$  ;
- 3R and 4R (the state 2),  $|r| \rightarrow 0.45 - 0.15 - 0.0$  .

So, cross correlation between the vectors of vibration signals at the said points is low, when  $|r| \rightarrow 0.3 - 0.2 - 0.02$ . However, cross correlation between the points 3R and 4R (the state 1) is considerably higher and the value of the correlation coefficient is the maximum  $|r| \rightarrow 0.7$ .

An important graphical expression of auto-covariance and cross-covariance functions for vibration signals of the second group is provided in Figs. 13–16. At Fig. 17, a graphical expression of the generalized (spatial) correlation matrix of the array of 8 vectors of vibration signals at 4 points in two states is provided.

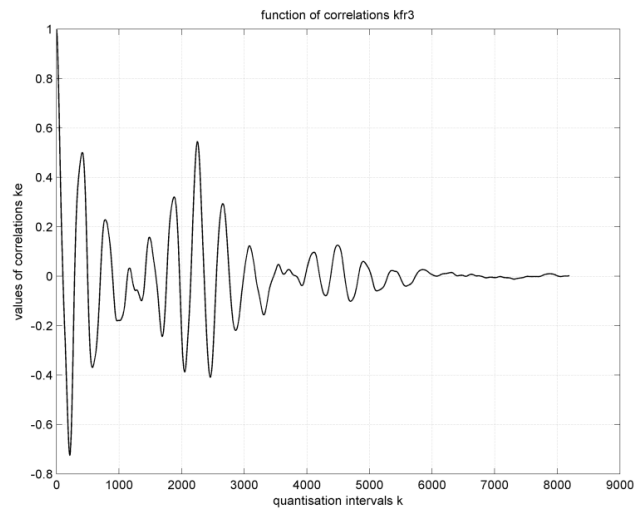


**Fig. 13** The normed auto-covariance function of vibration signals at the point 1P upon shock excitation

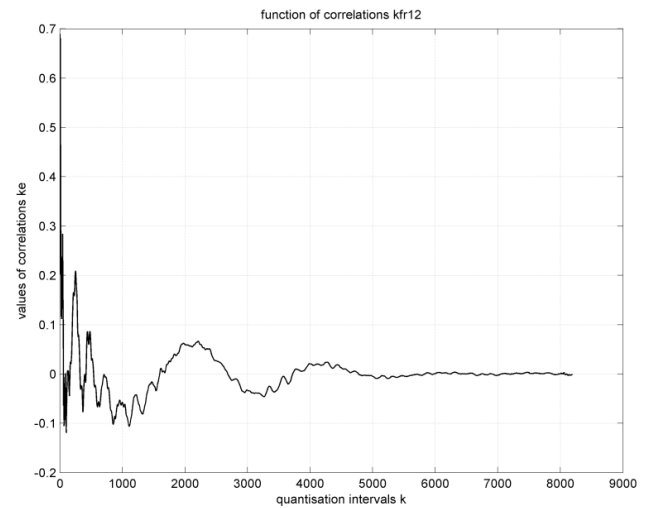


**Fig. 14** The normed cross-covariance function of vibration signals at the points 3R and 4R upon shock excitation

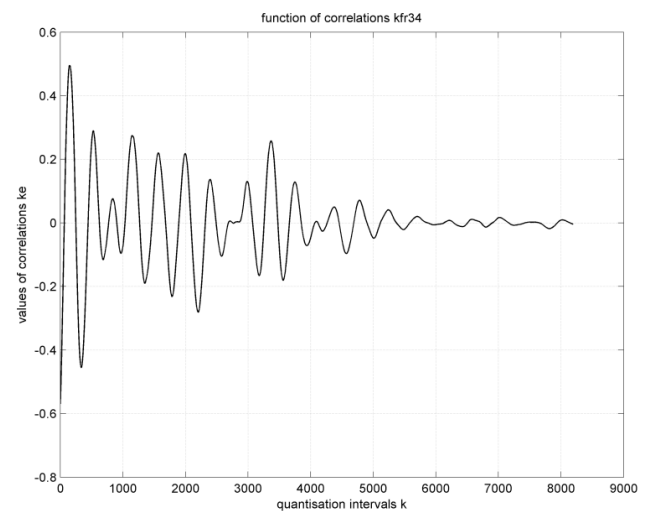


**Fig. 15** The normed cross-covariance function of vibration signals at the points 1P and 4P upon shock excitation

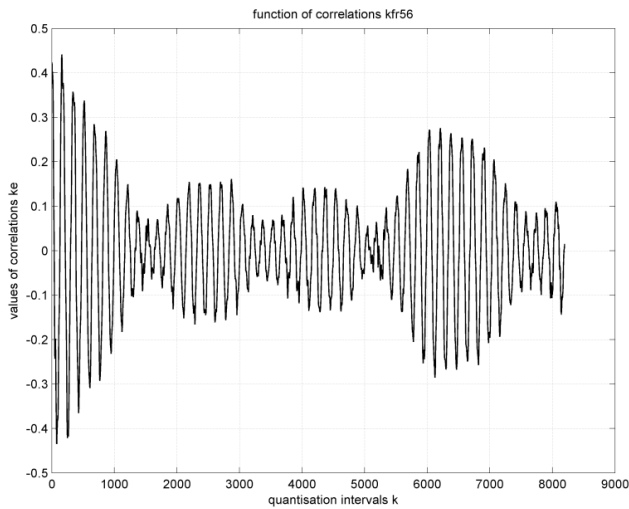


**Fig. 16** The normed cross-covariance function of vibration signals at the points 3R and 4R, when the engine is in operating state

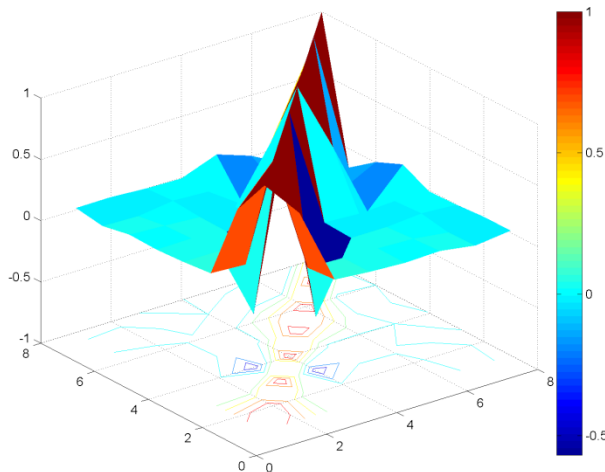


**Fig. 17** The graphical expression of the generalized (spatial) correlation matrix of the array of 8 vectors of vibration signals at 4 points of the vehicle, during two states.

## References

- Antoine, J. P. (2000) "Wavelet analysis of signals and images - A grand tour", *Ciencias Matemáticas*, 18(2), pp. 113–143.
- Dutkay, D. E.; Jorgensen, P. E. T. (2004) "Wavelets on fractals", *Revista Matematica Iberoamericana*, 22(1), pp. 131–180.  
<https://doi.org/10.4171/RMI/452>
- Eliason, E. M., McEwen, A. S. (1990) "Adaptive box filters for removal of random noise from digital images", *Photogrammetric Engineering and Remote Sensing*, 56(4), pp. 453–458.
- Hodouin, D., Flament, F. (1991) "Influence of data collection and conditioning strategies on the significancy of performance indices in mineral processing plants", In: *International Symposium evaluation and optimization of metallurgical performance*, Littleton, Colorado, USA, pp. 195–208.
- Horgan, G. (1998) "Wavelets for SAR images smoothing", *Photogrammetric Engineering and Remote Sensing*, 64(12), pp. 1171–1177.
- Hunt, B. R., Ryan, T. W., Gifford, E. A. (1993) "Hough transform extraction of cartographic calibration marks from aerial photography", *Photogrammetric Engineering and Remote Sensing*, 59(7), pp. 1161–1167.
- Kardoulas, N. G., Bird, A. C., Lawan, A. I. (1996) "Geometric Correction of SPOT and Landsat Imagery: A Comparison of Map and GPS-Derived Control Points", *Photogrammetric Engineering and Remote Sensing*, 62(10), pp. 1173–1177.
- Kilikevičienė, K., Skeivalas, J., Kilikevičius, A., Pečeliūnas, R., Bureika, G. (2015) "The analysis of bus air spring condition influence upon the vibration signals at bus frame", *Eksplotacija i niezawodność - Maintenance and reliability*, 17(3), pp. 463–469.  
<https://doi.org/10.17531/ein.2015.3.19>

## 4 Conclusions

1. The normed auto-covariance and cross-covariance functions of vibration signals at the preselected points of the vehicle enable the changes of correlation between the data vectors according to the quantization interval on the time scale. In the first group, the expressions of the normed auto-covariance functions of the vibration signals at the points of the mechanical structure in both states are of "undamped" periodic character because of traces of oscillations of the relevant harmonic. In the second group, the expressions of the normed auto-covariance functions of the vibration signals in both states are of low periodicity as well, when the estimates of the functions decrease from  $r \rightarrow 1.0$  to  $r \rightarrow 0.1-0$  at the values of quantization interval  $k \rightarrow 5000 (\tau_k \rightarrow 1.22 s)$ .
2. The normed cross-covariance functions of the first group become of irregular periodic character as well; the estimates of the function at any value of the quantization interval become low in both states and vary in the range  $|r| \rightarrow 0.5-0.2-0.01$ . The estimates of the normed cross-covariance functions of the second group become low at any value of the quantization interval in both states of the mechanical structure, when  $|r| \rightarrow 0$  at  $k \rightarrow 5000 (\tau_k \rightarrow 1.2 s)$ . The cross correlation of vectors of several vibration signals is higher when  $|r| \rightarrow 0.7-0.45$ .
3. Changes of the state of the vehicle frame impact changes of the intensity of vibration signals at the relevant points, and there is a cross correlation between them.

- Mah, R. S. H. (1990) "Process data reconciliation and rectification", In: Chemical process structures and information flows, Butterworth, Stoneham, USA, pp. 385–466.
- Narasimhan, S., Jordache C. (2000) "Data reconciliation and gross error detection - An intelligent use of process data", Gulf Publishing Company, Houston, TX, USA.  
<https://doi.org/10.1016/B978-0-88415-255-2.X5000-9>
- Romagnoli, J. A., Sanchez, M. C. (2000) "Data processing and reconciliation for chemical process operations", Academic Press, San Diego, USA.
- Skeivalas, J., Aleknienė, E., Gečytė, S. (2010) "Žemės dangos skaitmeninių vaizdų identifikavimo analizė" (Analysis of identifying the digital images of the earth's surface), Geodesy and Cartography, 36(4), pp. 146–150. (in Lithuanian)  
<https://doi.org/10.3846/gc.2010.23>
- Skeivalas, J., Jurevičius, M., Kilikevičius, A., Turla, V. (2015) "An analysis of footbridge vibration parameters", Measurement, 66, pp. 222–228.  
<https://doi.org/10.1016/j.measurement.2015.02.034>
- Skeivalas, J., Kizlaitis, R. (2008) "GPS skaitinių metodų taikymas elektrokardiogramų analizei" (Application of GPS Numerical Methods to the Analysis of Electrocardiograms), Geodezija ir kartografija, 34(4), pp. 127–133. (in Lithuanian)  
<https://doi.org/10.3846/1392-1541.2008.34.127-133>